ISBN: 978-3-95450-241-7 ISSN: 2673-5350 doi:10.18429/JACoW-IBIC2022-TUP15

NEW GAS TARGET DESIGN FOR THE HL-LHC BEAM GAS VERTEX PROFILE MONITOR

H. Guerin*,[1], R. De Maria, R. Kersevan, B. Kolbinger, T. Lefevre, M. T. Ramos Garcia, B. Salvant, G. Schneider, J. W. Storey, CERN, Geneva, Switzerland
S. M. Gibson, Royal Holloway, University of London, Surrey, UK
[1]also at Royal Holloway, University of London, Surrey, UK

Abstract

The Beam Gas Vertex (BGV) instrument is a novel non-invasive transverse beam profile monitor under development for the High Luminosity Upgrade of the LHC (HL-LHC). Its principle is based on the reconstruction of the tracks and vertices issued from beam-gas inelastic hadronic interactions. The instrument is currently in the design phase, and will consist of a gas target, a forward tracking detector installed outside the beam vacuum chamber and computing resources dedicated to event reconstruction. The transverse beam profile image will then be inferred from the spatial distribution of the reconstructed vertices. With this method, the BGV should be able to provide bunch-by-bunch measurement of the beam size, together with a beam profile image throughout the whole LHC energy cycle, and independently of the beam intensity. This contribution describes the design of the gas target system and of the gas tank of the instrument.

INTRODUCTION

With the foreseen High-Luminosity upgrade of the Large Hadron Collider (HL-LHC), knowledge of the beam emittance during the entire energy cycle will be critical for the machine commissioning. The Beam Gas Vertex (BGV) monitor being developed for this scope, proposes to use beam-gas inelastic hadronic interactions in order to provide a transverse beam size and beam profile measurement. As illustrated in Fig. 1, a noble gas is injected in a dedicated vacuum chamber to generate the beam-gas interactions. The tracks of issued secondary particles are detected by a forward tracking detector, located downstream of the gas target and outside the vacuum. Tracks and vertices are reconstructed with dedicated computing resources, and the beam size and profile are then inferred from the spatial distribution of reconstructed vertices. The instrument is being designed with the aim to achieve a beam size measurement accuracy $< 5\%$ and provide a bunch-by-bunch beam size measurement with a relative precision of a few percent within about 1 min, throughout the full energy cycle, and independent of the beam intensity.

A demonstrator device [1, 2] was installed and operated close to the Interaction Point 4 (IP4) of the LHC during Run 2 and demonstrated the feasibility of using beam-gas inelastic interactions to measure the beam size throughout the full LHC energy cycle and independently of the beam intensity, despite not being able to reconstruct interaction vertices. This limitation made the reconstruction of the beam profile impossible.

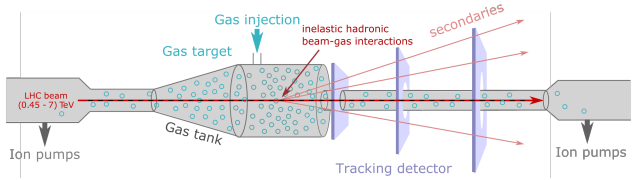

Figure 1: Sketch of the BGV instrument.

Following these results, work is ongoing to design the future instrument, which should be capable of vertexing to reach the above-mentioned specifications. A performance study based on Monte-Carlo simulation tools [3, 4] and track and vertex reconstruction analysis was carried out, in order to guide the BGV design.

The conclusions of this study lead to the choice of a compact tracker based on high resolution silicon pixel detectors. It was also decided to keep the distributed gas target system of the demonstrator, but to modify the dimensions of the vacuum chamber in order to reduce the longitudinal beam-gas interaction range and undesired radiation background, and to limit its beam impedance contribution in the LHC machine. This contribution presents the gas target and gas tank design of the future HL-LHC BGV instrument, and evaluates their impact on the machine operation.

GAS TARGET SYSTEM

Instrument Requirements

The BGV tracker was designed to detect tracks from inelastic beam-gas interactions occurring in a 1 m-long region along the beam axis and with an optimal distance of about 550 mm between the center of the gas target and the first detector plane. Most beam-gas interactions occurring outside this volume would not be used for the measurement and generate undesired background, increasing radiation levels in the LHC tunnel. Therefore, the requirements for the gas target design were to provide a uniform pressure distribution of about 1×10^{-7} mbar placed at the relevant distance from the tracker, with a quick pressure decrease outside it. Neon gas was chosen among other noble species in order not to saturate the chambers' non-evaporable getter (NEG) coating, and because remaining molecules after pumping wouldn't affect the sensibility of the leak detection systems, unlike helium and argon. Higher mass noble gases like krypton

* helene.chloe.guerin@cern.ch

ISBN: 978-3-95450-241-7 ISSN: 2673-5350 doi:10.18429/JACoW-IBIC2022-TUP15

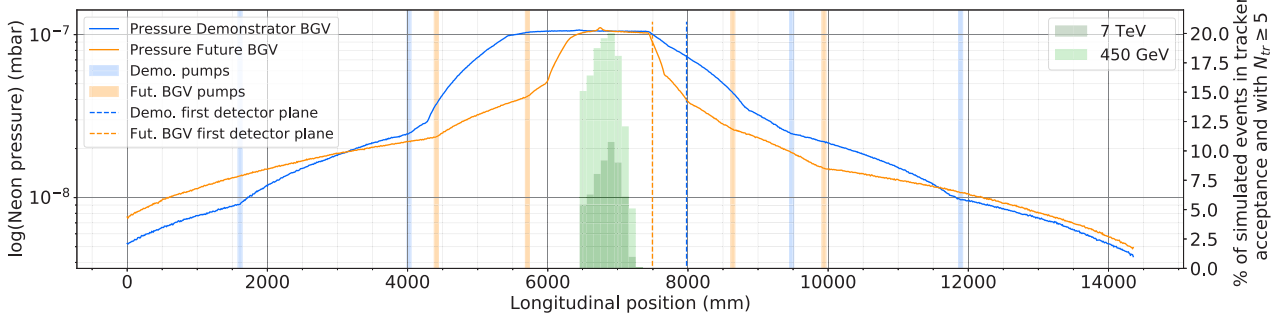

Figure 2: Longitudinal gas pressure profile of the BGV target during Ne injection, along the beam direction, as simulated with Molflow+ for both the demonstrator (blue) and future instrument (orange). The position of the ion pumps for the two designs are indicated by vertical lines of corresponding colours. Green bars show the percentage beam-gas interactions in the corresponding location, which can be reconstructed by the tracking detector (i.e. with a sufficient number of tracks N_{tr} in the tracker acceptance), at injection and flat top energies, based on Monte-Carlo simulations. The position of the first detector layer of each instrument is represented by the dashed vertical lines.

or xenon could also be considered in the future, but would require further vacuum studies.

Gas Injection System

The gas injection system proposed for the BGV has already been and is still being used in the LHC machine for other beam instruments including the demonstrator BGV [5], the Beam Gas Ionisation (BGI) monitor, and the Beam Gas Curtain (BGC) monitor [6]. As indicated in Fig. 1, the gas is injected via a capillary into the central, cylindrical part of the gas tank. The gas injected in the tank is purified with a commercial NEG filter, which reduces the concentration of contaminant from ppm to ppb level [7], and a valve allows to adjust the injected pressure. In the case of the BGV, two 500 L s^{-1} ion pumps are placed at each extremity of the central chamber, which is also surrounded by reduced aperture sections, to ensure a sharp decrease of the pressure outside the tank.

Longitudinal Gas Pressure Profile

The longitudinal gas profile of the BGV was simulated with the Molflow+ tool [8]. A parametric study of the tank dimensions was performed, starting from the demonstrator BGV setup, in order to understand how the shape of the tank and surrounding chambers impact the longitudinal gas profile. The length and diameter of each chamber and taper was considered, as well as the distance between the two pumps on each side and their proximity to the interaction chamber. The gas tank shape was thus optimised to provide a suitable pressure profile. The new longitudinal pressure profile is shown in Fig. 2, together with the one of the demonstrator. Compared to the demonstrator, the integrated pressure of the new configuration is reduced by 24%, which decreases the impact on the LHC radiation environment, while providing the required pressure in the region of interest for beam-gas interactions, at both injection and collision energies. Additional simulations, with the BGV setup included in the vacuum sectors of the foreseen locations, will be performed, as the proximity of cryogenic modules may affect the shape of the profile tails. The possible risk of Ne condensation and outgassing in cryogenic areas will also be assessed from these simulations.

GAS TANK DESIGN

The gas tank was designed taking the gas target needs into account, which were detailed in the previous section, and beam impedance and integration requirements, which are explained below. The new structure of the future instrument is shown in Fig. 3. The length and inner diameters of the different chamber parts are indicated, together with the position of the tracking detectors, first ion pumps and bellow.

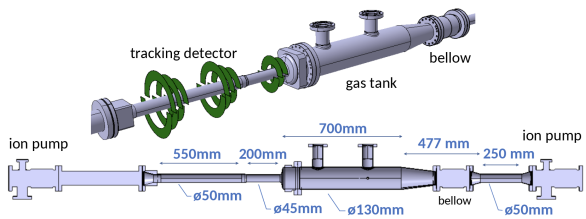

Figure 3: Most recent version of the HL-LHC BGV layout from CATIA [9] drawings.

Instrument Locations

The BGV instruments are foreseen to be installed on either side of the LHC IP4, where beam optics show little changes between injection and collision energies to facilitate beam parameters measurement, and with similar beam size in both transverse planes. The Beam 2 BGV is foreseen to be placed at the location currently occupied by the demonstrator BGV −220 m w.r.t IP4 center, where transverse β-functions cross at $\beta_x^{B2} \simeq 160$ m, and the Beam 1 instrument would be installed at +142 m w.r.t IP4 center, with a β-functions crossing of $\beta_x^{B1} \simeq 320$ m.

A critical parameter for the BGV performance is the diameter of the chamber downstream of the central gas chamber,

ISBN: 978-3-95450-241-7 ISSN: 2673-5350 doi:10.18429/JACoW-IBIC2022-TUP15

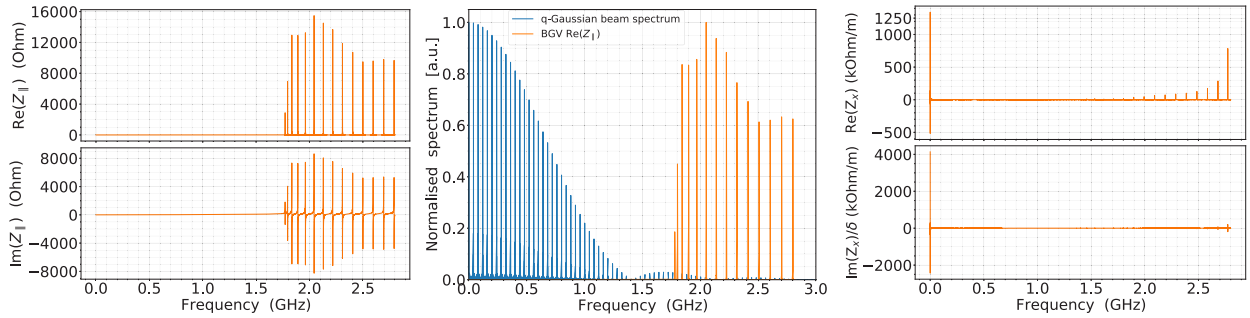

Figure 4: BGV beam coupling impedance simulated with CST Particle Studio. The real and imaginary longitudinal impedance spectrum are shown on the left figure and the transverse impedance spectrum on the right figure for the case of a transverse beam displacement of 12.5 mm. The middle plot shows the normalised beam spectrum for a q-Gaussian bunch shape, and normalised real longitudinal impedance, shifted in frequency to display the configuration with maximum dissipated power $P_{\text{loss}} = 40\,\text{W}$.

where the first detector layer is placed. Simulations have shown that most secondary particles have a small angle with respect to the beam axis, and particles with such trajectories also tend to have higher momenta, making them less prone to multiple scattering [3]. Minimising the detector beam pipe diameter is thus an important criterion in the optimisation of the tracker acceptance. At the locations foreseen for the two instruments, a beam pipe aperture of 45 mm inner diameter was agreed for the 200 mm-long chamber holding the first detector layer [10]. With such a small aperture, the chamber should be placed as close as possible to the β crossing point for the Beam 1 instrument and mechanical and alignment tolerances should be carefully considered.

Beam Coupling Impedance

Careful attention was given to the beam coupling impedance of the BGV gas tank, on the one hand because the contribution of the demonstrator was known to be non-negligible in the LHC machine [11], and on the other hand since beam instabilities due to impedance will increase with the beam intensity foreseen for HL-LHC.

A preliminary study [3] was performed with CST Particle Studio software [12], to understand how the design parameters of the gas tank impact its impedance. The main conclusions were that the diameter of the wide part of the tank is the most significant impact parameter, driving the frequency and shunt impedance of the main longitudinal resonant modes. With a longer gas tank, the number of these modes rises, but their shunt impedance also gets smaller. Finally, the taper sections can mitigate the impact of the resonant modes, but to a smaller extent compared to the two previous parameters.

Once the updated version of the tank shown in Fig. 3 was identified, its beam impedance was simulated with the wakefield solver of CST Particle Studio.

Longitudinal Impedance The real and imaginary part of the longitudinal impedance of the future gas tank design are shown in the left plots of Fig. 4. The pattern of the resonant modes is very similar to the one of the demonstrator structure [11], but with frequencies higher than 1.7 GHz (vs. >1.1 GHz for the demonstrator), and significantly smaller shunt impedance values (<16 kΩ), thanks to a smaller diameter of the wide part. The longitudinal effective impedance is obtained from the low frequency of the imaginary impedance: $Im(Z_{\parallel}/n) = 0.38\,\text{m}\Omega$. This value is almost twice smaller than the one of the demonstrator tank.

The expected power loss on the BGV was estimated based on Ohm's law, as described by Eq. (1), which considers the LHC beam of intensity I_{beam} and normalised spectrum Λ, and with the real part of the device impedance $\Re(Z_{\parallel})$. With discrete spectra, the power loss can be calculated as the sum of the contribution of each resonant mode coinciding with a beam harmonic, the fundamental being the bunching frequency $f_0 = 40\,\text{MHz}$.

$$P_{\text{loss}} = 2I_{\text{beam}}^2 \sum_{i=0}^{n} |\Lambda(\omega_i)|^2 \Re[Z_{\parallel}(\omega_i)] \,. \qquad (1)$$

The calculation was done with the most recent foreseen HL-LHC beam parameters [13], and with different bunch shapes. For each case, the impedance spectrum was shifted by a frequency varying between −20 MHz and 20 MHz, in order to consider all possible cases of overlap between the impedance resonant peaks and beam harmonics. For each bunch shape, the average power loss of all the frequency shift configurations is calculated, and the case with the maximum value is considered as worst possible configuration. Table 1 summarises the obtained results, listing for each bunch shape the average power loss value for the worst case parameters. The middle plot in Fig. 4 shows the normalised beam spectrum for a q-Gaussian bunch shape and the shifted real impedance spectrum of the BGV superimposed, in the worst case configuration. It is visible from this figure that the change of diameter of the tank shifted the impedance spectrum to higher frequencies when compared to the demonstrator, and therefore avoided the overlap with beam harmonics of relatively high intensity between 1.1 GHz and 1.5 GHz.

ISBN: 978-3-95450-241-7 ISSN: 2673-5350 doi:10.18429/JACoW-IBIC2022-TUP15

Table 1: Beam Induced Power Loss

Bunch shape	average P_{loss}	maximum P_{loss}
q-Gaussian	14 W	40 W
Gaussian	11 W	12 W
$\cos^2$	10 W	12 W

Transverse Impedance The transverse impedance of the HL-LHC BGV was simulated similarly. Since the BGV geometry modelled in CST is symmetrical with respect to the beam axis, the horizontal and vertical impedances are equivalent. Assuming the absence of transverse coupling between the two planes and neglecting terms of second and higher orders, the transverse impedance $Z_x(\omega)$ can be expressed as [14]: $Z_x(\omega) \simeq Z_x^0(\omega) + x_s Z_x^{\text{dip}}(\omega) + x_t Z_x^{\text{quad}}(\omega)$. A beam displacement x_s of 12.5 mm was simulated to estimate the dipolar (driving) term Z_x^{dip}, and a witness integration path displacement x_t of the same amount was simulated to derive the quadrupolar (detuning) term Z_x^{quad}. The zeroth order term $Z_x^0(\omega)$ was observed to be negligible based on simulations without offsets. The real and imaginary part of the total weighted transverse impedance are shown on the right plot of Fig. 4, weighted by the displacement $x_s = x_t = \delta$.

IMPACT ON LHC BEAM AND OPERATION

Operation Time and Radiation

When measuring beam size, the demonstrator BGV was operated with the gas profile shown in Fig. 2 and with an average plateau pressure of 1.4×10^{-7} mbar. This level was the same for both proton and ion runs, and the gas injection was usually turned on for multiple hours, and sometimes during most of the LHC energy cycle. Analyses of the total ionising dose rates and high energy hadron equivalent fluence in the vicinity of the demonstrator revealed that when turned ON, the BGV became the main source of radiation in this region [15]. An operation time of about 2 h per fill would be a minimum to measure beam size and emittance at the key phases of the energy cycle, including the ramp, and possibly calibrate the Beam Synchrotron Radiation Monitor (BSRT) at collision energy for longer measurements. Further studies are ongoing to estimate a maximum operation time, which will be limited by the radiation to the nearby active and passive instrument components.

Emittance Growth and Beam Half-Life Time

The BGV gas target is expected to have a negligible effect on the beam emittance and lifetime.

Considering first the beam particles' scattering on the gas target, and for a 1-σ beam size, the emittance growth per turn $\Delta\epsilon$ due to the presence of the BGV gas target can be calculated with Eq. (2), as detailed in Ref. [16]. In this formula, q_p is the charge number of the projectile, ie. of a proton in the beam, of momentum p and relativistic velocity β_r, and $\bar{\beta}_x$ represents the average transverse β-function along the gas target of length L. In the case of the BGV, the radiation length of the neon target is $L_{\text{rad, Ne}} \simeq L_{\text{rad, Ne, 1atm}}/(\bar{P}/1\text{ atmosphere}) = 1.2 \times 10^{13}$ m, where $\bar{P} = 2.72 \times 10^{-8}$ mbar is the average pressure along the gas target.

$$\Delta\epsilon = \frac{1}{2} q_p^2 \left(\frac{13.6\,\text{MeV}}{p\beta_r}\right)^2 \bar{\beta}_x \frac{L}{L_{\text{rad}}} \quad . \tag{2}$$

The normalised emittance growth rate $\Delta\epsilon_n$ can be expressed in $\mu\text{m}\,\text{h}^{-1}$ by scaling $\Delta\epsilon$ with the beam relativistic velocity β_r, Lorentz factor γ_L of the corresponding energy and with the LHC revolution frequency.

The resulting values are summarised in Table 2 for each beam at injection and collision energy. Emittance growth rates per fill of 0.16 % + 0.01 % = 0.17 % for Beam 1 and 0.08 % + 0.005 % = 0.085 % for Beam 2 are thus expected for the BGV operated for 1 h at injection and 1 h at collision energy. In the case where the gas injection would be turned ON several hours per fill, these values would stay way below the 10%-15% budget proposed for the beam size measurement in Ref. [17].

Table 2: Elastic Scattering Emittance Growth

Beam and Energy	$\Delta\epsilon$ (π rad m)	$\Delta\epsilon_n$ ($\mu\text{m}\,\text{h}^{-1}$)
Beam 1, 450 MeV	1.9×10^{-19}	3.2×10^{-3}
Beam 1, 7000 MeV	7.7×10^{-22}	2.0×10^{-4}
Beam 2, 450 MeV	9.3×10^{-20}	1.6×10^{-3}
Beam 2, 7000 MeV	3.8×10^{-22}	1.0×10^{-4}

In addition, calculating the beam lifetime with considering the rate of both elastic and inelastic interactions between beam protons and the BGV target molecules can gauge the amount of beam particles impacted by the gas target. Considering the new gas profile shown in Fig. 2, the half-life time of the HL-LHC proton beam would be 3 years. The impact of the BGV target on the beam lifetime can thus be considered negligible, similarly to the fraction of the beam protons interacting with the BGV target.

CONCLUSION

With the experience gained with the demonstrator BGV and with various simulation studies, a new gas target and gas tank designs are proposed for the HL-LHC BGV instrument. The impact of the BGV on the HL-LHC beam and operation was estimated based on simulation results, and will be smaller compared to the demonstrator, while ensuring the instrument's performance. The full design of the HL-LHC BGV will be detailed in a design report and presented in a review in October 2022.

ACKNOWLEDGEMENTS

The authors wish to thank Giuseppe Bregliozzi for his advises and feedback along the gas target design, together with the impedance working group for his support and comments regarding the gas tank impedance study. Thanks also to Daniel Prelipcean for his work on the radiation impact of the BGV.

ISBN: 978-3-95450-241-7 ISSN: 2673-5350 doi:10.18429/JACoW-IBIC2022-TUP15

REFERENCES

[1] A. Alexopoulos *et al.*, "Non-invasive LHC Transverse Beam Size Measurement Using Inelastic Beam-Gas Interactions," *Phys. Rev. Accel. Beams*, vol. 22, no. 4, p. 042 801, 2019. doi:10.1103/PhysRevAccelBeams.22.042801

[2] B. Wurkner, "Measurement of the LHC Beam Profile Using the Beam Gas Vertex Detector," Ph.D. thesis, Vienna, Tech. University, Germany, 2019.

[3] H. Guerin *et al.*, "The HL-LHC Beam Gas Vertex Monitor - Simulations for Design Optimisation and Performance Study," in *Proc. IPAC'21*, Campinas, Brazil, May 2021, pp. 2120–2123. doi:10.18429/JACoW-IPAC2021-TUPAB278

[4] B. Kolbinger *et al.*, "The HL-LHC Beam Gas Vertex Monitor - Performance and Design Optimisation Using Simulations," in *Proc. IBIC'21*, Pohang, Rep. of Korea, 2021, pp. 249–253. doi:10.18429/JACoW-IBIC2021-TUPP21

[5] G. Bregliozzi, V. Baglin, and P. Chiggiato, "Assessment of New Components to be Integrated in the LHC Room Temperature Vacuum System," 4 p, 2014. https://cds.cern.ch/record/1968548

[6] O. Sedlacek *et al.*, "HL-LHC Beam Gas Fluorescence Studies for Transverse Beam Profile Measurement," presented at IBIC'22, Kraków, Poland, Sep. 2022, paper TUP17, this conference.

[7] G. Bregliozzi, "Neon Venting of Activated NEG Beam Pipes in the CERN LHC Long Straight Sections without Losing Vacuum Performance," in *Proc. PAC'09*, Vancouver, Canada, May 2009, paper MO6RFP006, pp. 360–362. https://jacow.org/PAC2009/papers/MO6RFP006.pdf

[8] R. Kersevan and M. Ady, "Recent Developments of Monte-Carlo Codes Molflow+ and Synrad+," in *Proc. IPAC'19*, Melbourne, Australia, May 2019, pp. 1327–1330. doi:10.18429/JACoW-IPAC2019-TUPMP037

[9] *CATIA*. https://www.3ds.com/fr/produits-et-services/catia/

[10] R. D. Maria, private communication, 2022. https://indico.cern.ch/event/1164689/

[11] P. Hopchev *et al.*, "Beam gas vertex (bgv) demonstrator of a beam profile monitor in lhc," LHC-BGV-EC-0002, EDMS 1324635, 2014. https://edms.cern.ch/document/1324635/1.0

[12] *CST Microwave Studio*. http://www.cst.com

[13] R. Tomas Garcia *et al.*, "HL-LHC Run 4 proton operational scenario," CERN, Tech. Rep., 2022. http://cds.cern.ch/record/2803611

[14] S. Heifets, A. Wagner, and B. Zotter, "Generalized impedances and wakes in asymmetric structures," 1998. doi:10.2172/663316

[15] D. Prelipcean, "BGV beam-gas collisions at IR4 and related radiation levels and heat loads," 2022. https://indico.cern.ch/event/1129683/

[16] D. Möhl, "Sources of emittance growth," 2006. doi:10.5170/CERN-2006-012.45

[17] G. Arduini, A. Dabrowski, M. Lamont, J. Wenninger, and K. Wittenburg, "LHC Beam Size Measurement Review: Findings, comments and recommendations," 2019. https://indico.cern.ch/event/837340/